J Mater Sci (2009) 44:2021–2026
DOI 10.1007/s10853-009-3269-2

Microstructure and ionic conductivity of alternating-multilayer structured Gd-doped ceria and zirconia thin films

Yiguang Wang · Linan An · L. V. Saraf · C. M. Wang · V. Shutthanandan · D. E. McCready · S. Thevuthasan

Received: 14 April 2008 / Accepted: 13 January 2009 / Published online: 28 February 2009

Abstract Multilayer thin film of Gd-doped ceria and zirconia have been grown by sputter-deposition on α-Al_2O_3 (0001) substrates. The films were characterized using X-ray diffraction (XRD), atomic force microscopy (AFM), X-ray photoelectron spectroscopy (XPS), and transmission electron microscopy (TEM). The Gd-doped ceria and zirconia layers had the fluorite structure and are highly textured such that the (111) plane of the films parallel to the (0001) plane of the α-Al_2O_3. The epitaxial relationship can be written as $(111)_{ZrO_2/CeO_2}//(0001)_{Al_2O_3}$ and $[11-2]_{ZrO_2/CeO_2}//[-2110]_{Al_2O_3}$, respectively. The absence of Ce^{3+} features in the XPS spectra indicates that the Gd-doped ceria films are completely oxidized. The ionic conductivity of this structure shows great improvement as compared with that of the bulk crystalline material. This research provides insight on designing of material for low temperature electrolyte applications.

Y. Wang
National Key Laboratory of Thermostructure Composite Materials, Northwestern Polytechnical University, Xi'an 710072, China

Y. Wang (✉) · L. An
College of Engineering and Computer Science, University of Central Florida, Orlando, FL 32816, USA
e-mail: wangyiguang@nwpu.edu.cn

L. V. Saraf · C. M. Wang · V. Shutthanandan · D. E. McCready · S. Thevuthasan (✉)
Enviornmental Molecular Sciences Laboratory, Pacific Northwest National Laboratory, Richland, WA 99352, USA
e-mail: theva@pnl.gov

C. M. Wang
e-mail: chongmin.wang@pnl.gov

Introduction

The operation of all solid-state electrochemical devices including batteries, sensors, fuel cells, and oxygen pumps is essentially built on ion conduction in solid electrolytes. The operation of solid oxide fuel cell (SOFC) is rather simple, however, there are several scientific issues associated with oxide electrolytes, anodes, and cathodes. Since the oxide electrolytes are crucial components of the SOFCs, fundamental understanding of oxygen transport behavior in these electrolytes [1, 2] has been the interest of research community for decades due to the need for development of a better electrolyte material. The most advanced SOFCs employ oxygen-ion conducting zirconia based electrolytes, specifically, yttria stabilized zirconia (YSZ). The ionic conductivity of the electrolyte determines the operation temperature of the cell, which is currently around 1275 K [3]. The high temperature operation of SOFCs currently on the market is significantly restricted by the materials that meet the performance requirement of the cell. For example, in order to improve the oxidation resistance of the stainless-steel interconnect, it needs to be coated using a layer of oxidation resistance material. This inevitably hinders the development and commercialization of the SOFCs because of the cost associated with the modification of the materials. One of the strategies to resolve the oxidation problem is to develop solid-oxide electrolyte that allows the cell to be operated at a relatively lower temperature, which requires the enhancement of the ionic conductivity of the electrolyte at a relatively low temperature. The prevalent approach to enhance the ionic conductivity of the electrolyte is based on the incorporation of different dopants, which preferentially increase the concentration of certain types of lattice defects in the electrolytes [4]. This strategy shows promising results, but is not always sufficient.

It has been generally realized that microstructural design may lead to an enhanced ionic conductivity. For example, it has been demonstrated that use of thin YSZ films, as contrast to the conventional bulk YSZ material, may lead to a higher ionic conductivity [5]. On the other hand, reducing the thickness of the electrolyte layer will not necessarily lead to an operation temperature of lower than 900 K [5]. Ceria-doped with a divalent or trivalent oxide (mostly gadolinia or samaria) have been found to exhibit a higher ionic conductivity than YSZ at lower temperatures and a lower conduction activation energy [5–10]. The major issue with this material is that it gains considerable electronic conductivity when exposed to the reducing atmospheres at temperatures above 1025 K, leading to voltage loss.

It is well-known that nanoscale materials often display properties that are very different from the coarse-grained bulk materials. In particular, it has been recently demonstrated that a nanoscale lamellar structure of two different fluorides (calcium fluoride and barium fluoride) can exhibit significantly higher ionic conductivity along the interfacial directions at moderate temperatures [11]. Azad et al. [12] have reported the enhancement of oxygen ionic conductivity of Gd-doped multi-layer CeO_2/ZrO_2 films, which is attributed to the nano-size effect of the multi-layer thin film. They observed that the increase in oxygen ionic conductivity is a function of the number of layers when the total thickness of the film was kept as a constant. The conductivity measured on the multi-layer films are significantly higher than that of either single crystal YSZ thin film or polycrystalline YSZ, or trivalent element doped ceria.

In this study, Gd-doped ceria and zirconia multi-layers films were deposited using sputter deposition method, which is an industrially friendly method and viable for a large area preparation of the material. The objective of this research is to explore the feasibility of synthesizing high quality multi-layer thin films of Gd-doped ceria and zirconia with a larger thickness than that obtainable with oxygen plasma assisted MBE. The films were characterized by the bulk and surface sensitive characterization techniques, which include Rutherford backscattering spectrometry (RBS), X-ray diffraction (XRD), X-ray photoelectron spectroscopy (XPS), atomic force microscopy (AFM), and cross-sectional high resolution transmission electron microscopy (HRTEM).

Experiment

The films were grown on the α-Al_2O_3 (0001) substrate using the sputter deposition system at the Environmental Molecular Sciences Laboratory (EMSL) of Pacific Northwest National Laboratory. Zirconium was sputtered from the target using RF sputtering while cerium and gadolinium were sputtered using DC sputtering in the same sputtering chamber. The background pressure in the chamber was kept at 8×10^{-3} torr and a mixture of O_2/Ar was used as sputter gas with 10 sccm Ar and 3 sccm O_2. The deposition rate was calibrated using RBS measurement of the film thickness. The deposition rate for ZrO_2 and CeO_2 were about 0.24 nm/min, and 0.6 nm/min, respectively. The XPS measurements were performed in order to investigate the surface properties and the charge state of cations in the films. Cross-sectional high resolution transmission electron microscopy (HRTEM) imaging and selected area electron diffraction were used to characterize the structure of the film. TEM sample preparation was done using a standard tripod wedge polishing method followed by Ar^+ ion beam thinning to electron transparency. X-ray diffraction measurements were recorded using a Phillips X'pert $\theta - 2\theta$ diffractometer at 40 kV and 50 mA followed by data analysis using JADE 6.0 program. To determine the orientation(s) of the film, X-ray pole figures were collected for the film (220) reflections. In this pole, the strong reflection from the substrate is minimized. Surface morphology was examined by AFM. The total conductivity measurements were carried out using a four-probe van der Pauw technique.

Results and discussion

X-ray diffraction results from the 50-layer film (nominal thickness $\sim$2 micron) are presented in Fig. 1. These results clearly indicate that these films are composed of Gd-doped ceria and zirconia. In the spectrum, the strong narrow peaks correspond to the Al_2O_3 (0001) substrate. Both Gd-doped ceria and zirconia exhibit single phase with a preferred orientation of (111) plane that parallel to the (0001) of the α-Al_2O_3. In comparison to the reference data of ceria and zirconia [13, 14], the peaks associated with Gd-doped ceria and zirconia are shifted to lower 2θ values

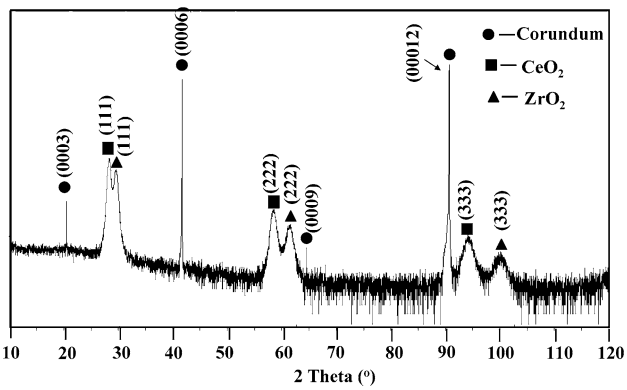

Fig. 1 XRD pattern of Gd-doped zirconia and ceria multi-layer thin film

due to the doping of Gd in the films. The lattice expansions for both Gd-doped ceria and zirconia determined from XRD are approximately 0.92% and 1.97%, respectively. Significantly larger lattice expansion for Gd-doped zirconia was expected since the ionic radius of gadolinium atom (0.94 Å) are only slightly larger than that of cerium atom (0.92 Å), but is significantly larger than that of zirconium atom (0.79 Å). Different degree of lattice expansion caused by the gadolinium doping of zirconia and ceria will lead to a reduced lattice mismatch, δ, across the interface between zirconia and ceria layers. δ is normally defined as: $\delta = (a_{Ce} - a_{Zr})/a_{Zr}$, where a_{Ce} and a_{Zr} are the lattice constants of the ceria and zirconia, respectively. Using the reference lattice values of 0.5411 nm for ceria and 0.5128 nm for c-zirconia, a δ value of 5.5% can be obtained. The δ value determined from the XRD results is approximately 4.4%.

To further investigate the epitaxial growth orientation of the thin films, pole figures were collected for both zirconia and ceria as presented in Fig. 2. The peak originated from (220) reflections was used to collect this data. The results clearly demonstrated that both Gd-doped ceria and zirconia layers possess a single domain structure with a preferred orientation of (111) plane parallel to the (0001) of α-Al_2O_3.

The surface morphologies of the films were characterized by the atomic force microscopy (AFM). In these experiments, the films with a total thickness of 240 nm were characterized, intending to obtain the surface morphology with respect to the film growth temperature and individual layer thickness. The AFM images shown in Fig. 3a and b represent the surface morphology of a 10 layer film (a) and a 32 layer film (b), respectively, both of which were grown at 600 °C. Figure 3c shows the surface morphology of a 10 layer film deposited at room temperature. Figure 3 clearly demonstrates that the 10 layer film deposited at room temperature (Fig. 3c) shows the largest surface roughness as compared to that grown at 600 °C (Fig. 3a). In addition, the surface roughness appears to be

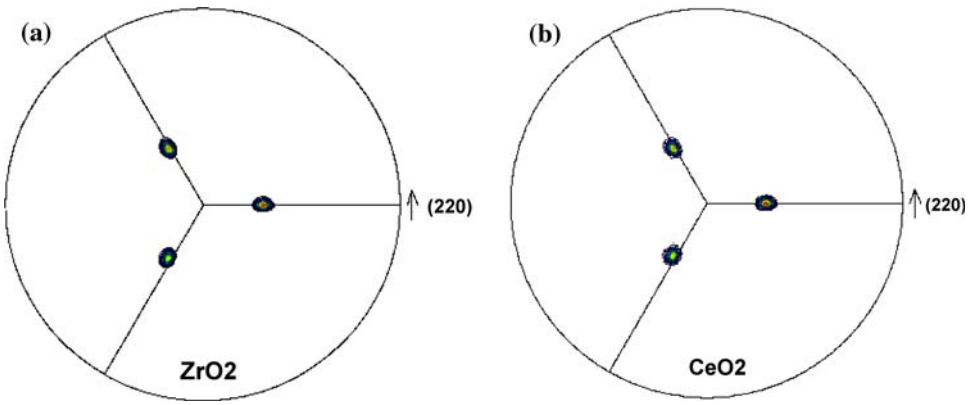

Fig. 2 Pole figures of the Gd-doped zirconia and ceria multi-layer thin film. The reflection pole is (220) for both ceria and zirconia

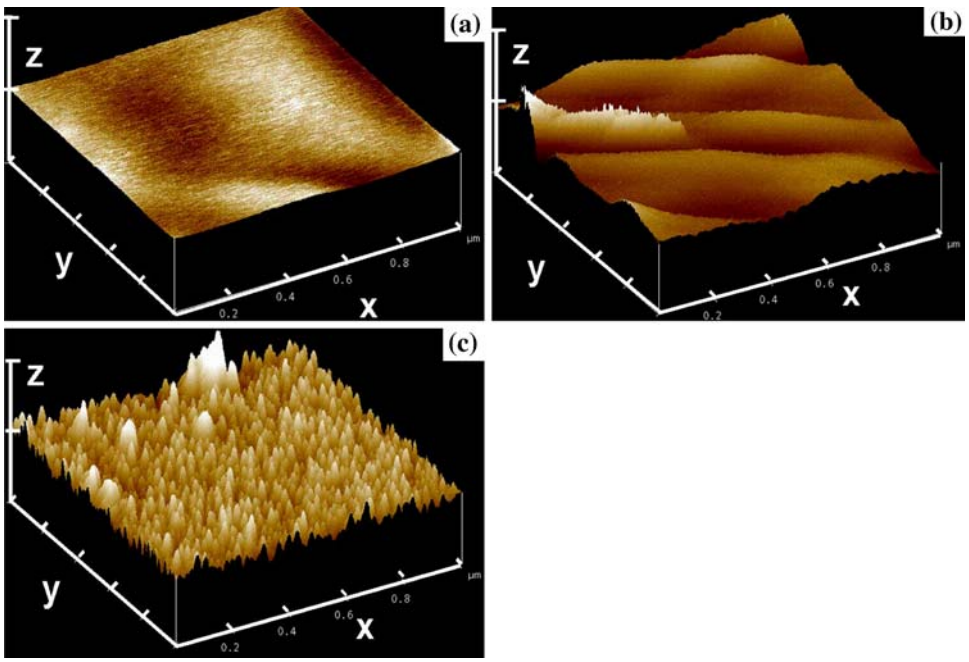

Fig. 3 AFM images showing the surface morphology of the Gd-doped zirconia and ceria multilayer thin films. **a** The 10 layer thin film deposited at 600 °C, **b** The 32 layer thin film deposited at 600 °C, and **c** The 10 layer thin film deposited at room temperature (x, y direction: 0.2 μm/div; z direction: 10 nm/div)

large in the 32 layer film (Fig. 3b) as compared to the 10 layer one grown at 600 °C (Fig. 3a). These results indicate that films deposited at low temperature have a larger surface roughness than that grown at high temperatures. Energetically, a rough surface corresponds to the high energy state, indicating that the film deposited at a lower temperature corresponds to an overall high energy state. Dependence of the surface roughness on the deposition temperature can be generally explained from the point of view of surface diffusion of the atoms. At low temperature, the surface diffusion of the atoms is so slow such that the atoms on the surface cannot rearrange themselves to lead to a smoother surface, which corresponds to a lower surface energy configuration. On the other hand, at a higher temperature, the diffusion of the atoms on the surface is fast, which is a process that leads to the smoothening of the surface, therefore lowering the overall energy of the system. As a result, the films grown at a higher temperature shows a smooth surface as compared with those grown at room temperature. However, it appears that, films deposited at the same temperature, with the increase of the layers, the surface roughness increases as demonstrated by comparing Fig. 3a and b. Two factors may be suggested to explain this. First, it is related to the strain in the film. For a thinner film, the strain originated from the interface may extend to the top of the film, therefore restricting the movement of atoms on the top layer of the film. Secondly, due to the lattice mismatch between ceria and zirconia layers, the defect originated from the interface may propagate through each layer of the film. This may lead to a situation that the top layers will be more defective than the bottom layers, therefore giving a high surface roughness on the top layer when a thicker film was deposited. As a result, the roughness on the 32 layer film surface appears to be more, in comparison to that on the 10 layer film.

Cross-sectional TEM images of the 10 layer alternating Gd-doped zirconia and ceria multilayer film are shown in Fig. 4. It can be seen that the Gd-doped ceria and zirconia approximately have the same thickness for each layer, which is $\sim$24 nm. The selected area electron diffraction pattern (SAED) shown in Fig. 4b indicates that the layers of both ceria and zirconia have the same orientation with respect to the α-Al_2O_3 substrate, which is consistent with the results of the XRD spectra and X-ray pole figure analysis. The orientation relationship between the film and the substrate can be written as $(111)_{ZrO_2}//(111)_{CeO_2}//(0001)_{Al_2O_3}$ and $[11-2]_{ZrO_2}//[11-2]_{CeO_2}//[-2110]_{Al_2O_3}$, respectively. The lattice constant mismatch between the Gd-doped zirconia and ceria can be seen from the spots splitting at a high diffraction order.

The charge states of the cerium and zirconium in the film were determined using X-ray photoelectron spectroscopy (XPS) (Fig. 5). There is no significant difference between the binding energies associated with Ce $3d_{7/2}$ and Ce $3d_{5/2}$ from the Gd-doped ceria film and pure ceria film discussed in a previous paper [15]. In addition, the absence of the features associated with the Ce^{3+} valence state indicates that the Ce in the film is fully oxidized to Ce^{4+}. For zirconia layer, the XPS spectrum shown in Fig. 5b clearly indicates the valence state of Zr^{4+}.

The total conductivity, which consists of the sum of the electronic and oxygen ionic conductivity in these layered

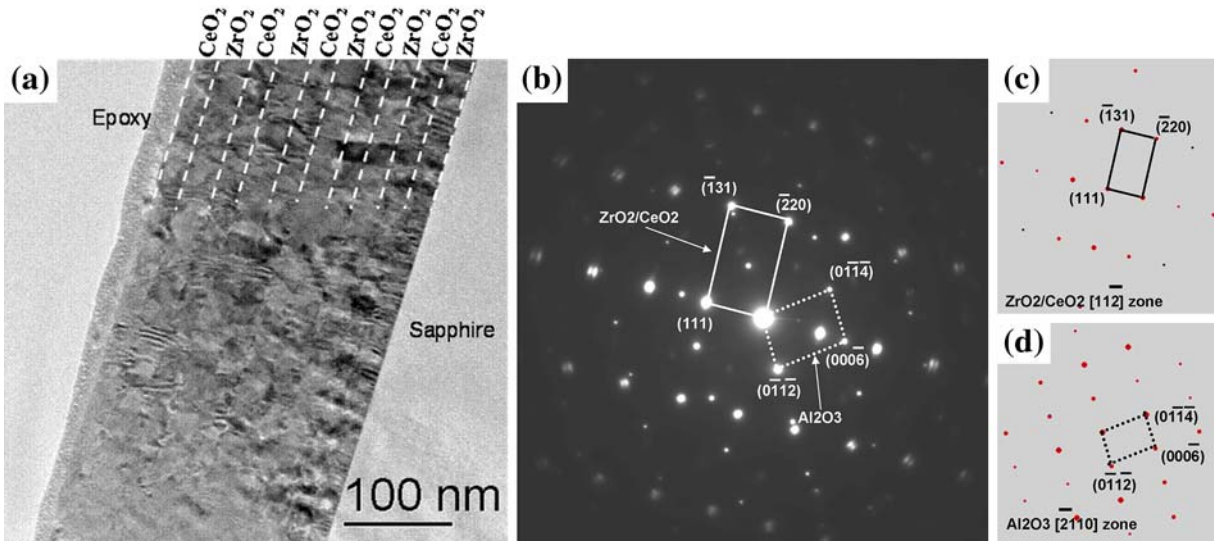

Fig. 4 **a** Cross-sectional TEM images of the 10 layer alternating Gd-doped zirconia and ceria multilayer thin film. **b** Selected area electron diffraction pattern of the film with the basic diffraction vectors indicated for CeO_2/ZrO_2 and α-Al_2O_3. **c** the schematic of the diffraction pattern of CeO_2/ZrO_2 from [11–2] zone axis. **d** the schematic of the diffraction pattern of α-Al_2O_3 from [−2110] zone axis

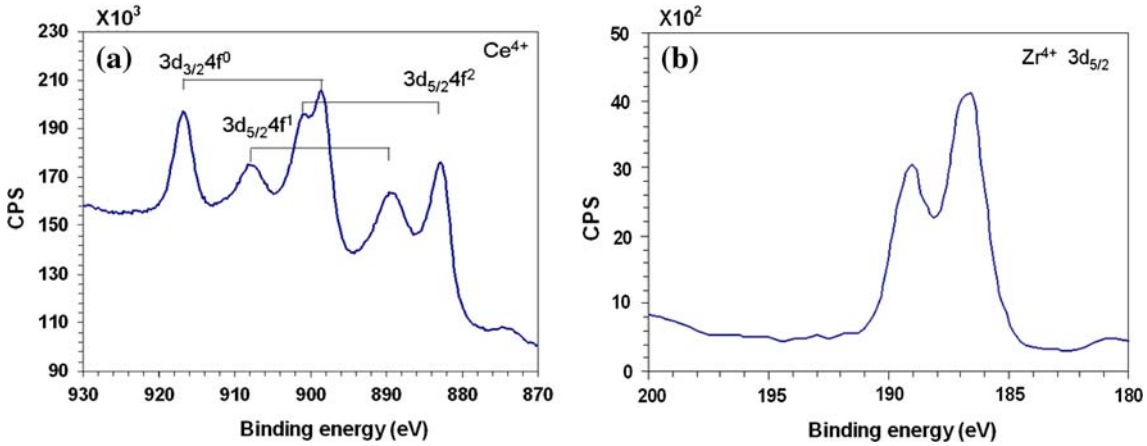

Fig. 5 XPS spectra of CeO_2 (**a**), and ZrO_2 (**b**). The brackets in (**a**) show the spin orbital pairs (5/2 and 3/2) for Ce^{4+}

films, was measured as a function of temperature using a four-probe van der Pauw technique [16]. It is generally believed that the electronic conductivity in these oxides is significantly small as compared with the ionic conductivity [6]. This is especially true for the low temperature regime. Therefore, it can be generally believed that the total conductivity measured on these films is dominated by the oxygen ionic conductivity [6]. Consequently, the total conductivity will be identified as oxygen ionic conductivity throughout this paper. The ionic conductivity of alternating Gd-doped ceria and zirconia films of 50 layer is shown in Fig. 6. Compared with single crystalline zirconia film [5] and Gd-doped polycrystalline ceria [6], the alternating-multilayer structure shows a significantly higher oxygen ionic conductivity, especially at the low temperature regime. These results are consistent with the results obtained from the multilayer structures generated using oxygen plasma assisted MBE method [12]. From the Arrhenius plots of the oxygen ionic conductivity as a function of temperature, the activation energy for ionic conductivity can be calculated as 0.83 eV, which is lower than that of 1.04 eV for single crystalline YSZ, and 0.97 eV for Gd-doped ceria. The physical reason for the enhanced ionic conductivity of the multi-layer structured film has been postulated to be related to the interface structure of the film as detailed in references [11] and [12]. This aspect of work is not pursued in this work.

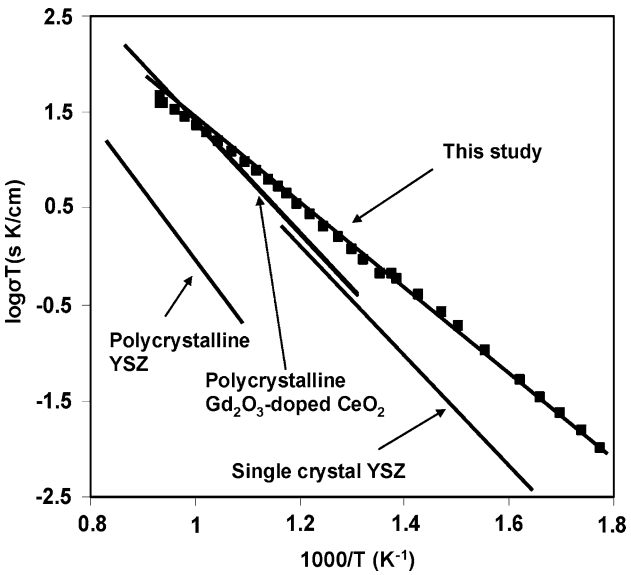

Fig. 6 Arrhenius plots of oxygen ionic conductivity of 50 layer Gd-doped zirconia and ceria multilayer thin film. The data from the polycrystalline bulk YSZ [5], polycrystalline bulk Gd-doped ceria [5], and single crystal YSZ film [6] are also shown for comparison

Conclusions

High quality multilayer thin film structures of alternating Gd-doped ceria and zirconia were prepared by the sputter deposition method. The films show highly textured structure such that the (111) planes of both the ceria and zirconia are parallel with the (0001) of the α-Al_2O_3 substrate. The surface roughness of the film shows dependence on the total thickness, number of layers, and the deposition temperature. Typically, films deposited at a higher temperature normally possess a smooth surface as compared with that deposited at room temperature. The multi-layer structured films shows a high ionic conductivity as compared with that of the correspondingly bulk crystalline material of similar composition.

Acknowledgements The research described in this paper was performed in the Environmental Molecular Sciences Laboratory, a national scientific user facility sponsored by the US Department of Energy's Office of Biological and Environmental Research and located at Pacific Northwest National Laboratory (PNNL), which is operated by Battelle for the DOE under Contract No.

DE-AC06-76RLO-1830. Y. Wang would like to acknowledge the support of the physical and chemical fellowship of PNNL that enables this work was done.

References

1. Minh NQ (1993) J Am Ceram Soc 76:563
2. Yamamoto O (2000) Electrochim Acta 45(15–16):2423
3. Ralph JM, Schoeler AC, Krumpelt M (2001) J Mater Sci 36(5):1161. doi:10.1023/A:1004881825710
4. Steele BCH (1996) Curr Opin Solid State Mater Sci 1(5):684
5. Ikeda S, Sakurai O, Uematsu K, Mizutani N, Kato M (1985) J Mater Sci 20(12):4593. doi:10.1007/BF00559349
6. Minh NQ, Takahashi T (1995) Science and technology of ceramic fuel cells. Elsevier, Amsterdam, p 94
7. Yahiro H, Eguchi Y, Eguchi K, Arai H (1988) J Appl Electrochem 18(4):527
8. Steele BCH (2000) Solid State Ionics 129(1–4):95
9. Kudo T, Fueki K (1990) Solid state ionics. Kodansha Ltd., Tokyo and VCH Publisher, New York, p 1
10. Maier J (1995) Prog Solid State Chem 23(3):171
11. Sata N, Eberman K, Ebert K, Maier J (2000) Nature 408(6815):946
12. Azad S, Marina OA, Wang CM, Saraf L, Shuttanandan V, McCready DE, EI-Azab A, Jaffe JE, Engelhard MH, Peden CHF, Thevuthasan S (2005) Appl Phys Lett 86:131
13. Powder Diffraction File Database, The International Centre for Diffraction Data. Newtown Square, PA, PDF 2002, 49-1642
14. Powder Diffraction File Database, The International Centre for Diffraction Data. Newtown Square, PA, PDF 2002, 34-0394
15. Kim YJ, Thevuthasan S, Shutthananadan V, Perkins CL, McCready DE, Herman GS, Gao Y, Tran TT, Chambers SA, Peden CHF (2002) J Elec Spectr Rel Phen 126(1–3):177
16. van der Pauw LJ (1958) Philips Res Rep 13:1